ACCOUNTS
of chemical research

Advances in Laser Cleaning of Artwork and Objects of Historical Interest: The Optimized Pulse Duration Approach

SALVATORE SIANO* AND RENZO SALIMBENI
Istituto di Fisica Applicata "Nello Carrara", Consiglio Nazionale delle Ricerche, Sesto Fiorentino (Florence), Italy

RECEIVED ON JULY 8, 2009

CONSPECTUS

Laser ablation has found numerous applications in biomedical and industrial settings but has not spread as quickly as a means of cleaning artwork. In this Account, we report recent advances in the study and application of laser cleaning to the conservation of cultural heritage. We focus on the solution of representative cleaning problems of encrusted stones, metals, and wall paintings that were achieved through the optimization of laser pulse duration.

We begin by introducing the basic mechanisms involved in the laser ablation of stratified materials and the criteria for preventing undesired side effects to the substrate and then briefly present case studies for each of these materials. Laser interaction effects are reviewed in a schematic way, with a concise overview of the physical models needed to support intuitive interpretations of the phenomenology observed, both in laboratory tests and in practical applications on important artifacts. This approach aims to provide keys of generalization that will favor the rigorous application of laser cleaning, repeatability of the successful results reported in this work, and further dissemination and acceptance of the technique.

The topics treated examine the ablation mechanisms along with the efficiency, gradualness, selectivity, and effectiveness of the technique as a function of the pulse duration of neodymium laser systems and the operating conditions. Physical modeling and experimental evidence support the selection of pulse durations of between several tens of nanoseconds and several tens of microseconds, making it possible to minimize the risk of photothermal and photomechanical effects and maximize the selectivity of the ablation process.

The sections dedicated to stones and metals also deal with the important problem of discoloration, which has significantly slowed the spread of the laser cleaning technique. The well-known problem of a yellowish appearance after laser cleaning is shown to be closely related to the ablation process; it can therefore be prevented by a suitable selection of irradiation parameters. The metal surfaces investigated are amalgam gilding, gold leaf gilding, and, for the first time, silver artifacts. We also describe the criteria used for applying laser ablation techniques to restoring unique masterpieces, such as Lorenzo Ghiberti's *Porta del Paradiso* and Donatello's *David*. Furthermore, a novel and unusual cleaning approach for archaeological silver is reported. Based on underwater laser irradiation, it provides a way to prevent oxidative effects and amplify the photomechanical coupling to the hard, thick concretions that usually accompany archaeological pieces.

Finally, the experimental extension of the laser cleaning approach to wall painting and its practical use in important restoration works is presented. The practical examples reveal a significant advance in perspective for the application, which was unthinkable until recently. In sum, this Account describes novel technological and methodological contributions of laser cleaning that are having a significant impact in the field of cultural heritage conservation.

1. Introduction

Despite the laser cleaning of artworks being introduced about 10 years before industrial and biomedical applications of laser ablation[1] and many successful studies having been reported,[2] the dissemination of this technique is proceeding relatively more slowly than the latter applications. The

Published on the Web 01/28/2010 www.pubs.acs.org/acr
10.1021/ar900190f

main obstacles to a rapid spread arise from the difficulty in suitably addressing a variety of complex cleaning problems, which involve material stratifications that have variable physical and chemical properties. In principle, the optimization of the laser cleaning of artwork is much more complex than any other application of laser ablation. Furthermore, the degree of cleaning to be achieved can be univocally defined only in some cases, whereas it is often the result of intertwined multidisciplinary factors including objective material assessments, fruition expectations, intrinsic limits of the methodology, the skilfulness of the restorer, and others.

During the past decade, we have provided substantial evidence that the laser pulse duration is the most crucial parameter. A careful optimization allows achieving high gradualness and selectivity in stone and metal cleaning, which is producing a significant application impact. During the 1990s, a novel fiber-coupled Nd:YAG (1064 nm) emitting pulses of 20 μs, the so-called short free running (SFR) temporal regime, was introduced.[3] This pulse duration domain can provide unique gradualness and self-termination performances. As a result of its successful experimentation, two versions emitting pulses with a duration between 40 and 150 μs (1−2 J/pulse) were marketed several years ago, as alternatives to the most commonly used Q-switching (QS) Nd:YAG laser emitting pulses of 5−20 ns (0.1−1 J/pulse).

More recently, a contribution for extending the application of laser cleaning to metal surfaces has been provided. The state of the art on this topic was in its very early stages until the beginning of the past decade, when we started investigating the conservation problems of Ghiberti's *Porta del Paradiso*.[4] The study proved the need and advantages of using pulse durations of several tens of nanoseconds and supported the overall application of laser cleaning to the friezes of the wings. A special Nd:YAG laser with a pulse duration of 70 ns known as long Q-switching (LQS) was developed for performing this important conservation treatment.[5]

As one of the main consequent follow-ups, two years ago a novel, LQS Nd:YAG laser (120 ns) was marketed. Meanwhile, the effectiveness of the SFR has been proven also for gold leaf gilding. Finally, both temporal regimes began to be tested to clean wall paintings.

Evidence of the apropriateness of the approach have emerged from new systematic investigations and case studies. In this Account, we present the most recent methodological advances achieved in the laser cleaning of stones, metals, and wall paintings, based on suitable selections of the laser pulse duration and irradiation conditions.

2. Stones

Extensive applications of laser cleaning were carried out on marble and limestone.[6] Up until recent years, mostly QS lasers were used for this purpose. There were essentially two limitations that provided room for proposing longer pulse duration: the occurrence of surface damage to the substrate at relatively low operative fluences, especially in cases of strong decohesion, and the recurrent yellowish appearance of the surface uncovered. The longer pulse duration allows overcoming these problems, although it reduces the efficiency.

2.1. Ablating with Different Laser Pulse Durations. The dependence of the ablation rate, z_{ab} (μm/pulse), on the laser pulse duration (t_L) was systematically investigated through ablation tests carried out on laboratory samples that simulated typical black crusts on stones. The samples were prepared by applying the following mixture on sandstone substrates: 60% gypsum, 30% quartz powder, 8% carbon black, and 2% burnt sienna. Cross-section examinations showed fairly homogeneous distributions of the inert component and pigment load within the gypsum matrix.

Reflectance and transmittance measurements using an integrating sphere enabled us to estimate the optical penetration at 1064 nm ($\delta \cong 27$ μm), through the fitting of the transmission fluence, $F(z) = F_a e^{-z/\delta}$, where F_a is the absorption fluence. It is much lower than the whole thickness of the crust, which makes the following considerations on ablation rates of general valence at least in stone cleaning.

Ablation tests were carried out using three Nd:YAG lasers systems: QS, LQS, and SFR at a pulse repetition frequency of 2 Hz. The surface under treatment was humidified with nebulized water at the same repetition frequency. Lastly, z_{ab} values associated with different fluences and pulse durations have been determined through the measurement of the depth (d_{ab}) produced by a number of laser pulses (n_p) using a contact microprofilometer ($z_{ab} = d_{ab}/n_p$).

The experimental ablation plots achieved are shown in Figure 1. They can be interpreted with the help of the so-called *blow-off* model. This was formerly introduced for describing vaporization-mediated ablation of homogeneous materials, but it can easily be adapted to the present heterogeneous crust. The model assumes that the material removal begins above a characteristic threshold, $F_{th} = \delta\varepsilon_{cr}$, where ε_{cr} is the average critical energy density (J/cm^3), which provides the following scaling law: $z_{ab} = \delta \ln(F/F_{th})$. The saturation of the ablation rate is defined by the equation $z_{ab} = \delta$, which occurs at $F = F_s = eF_{th}$.

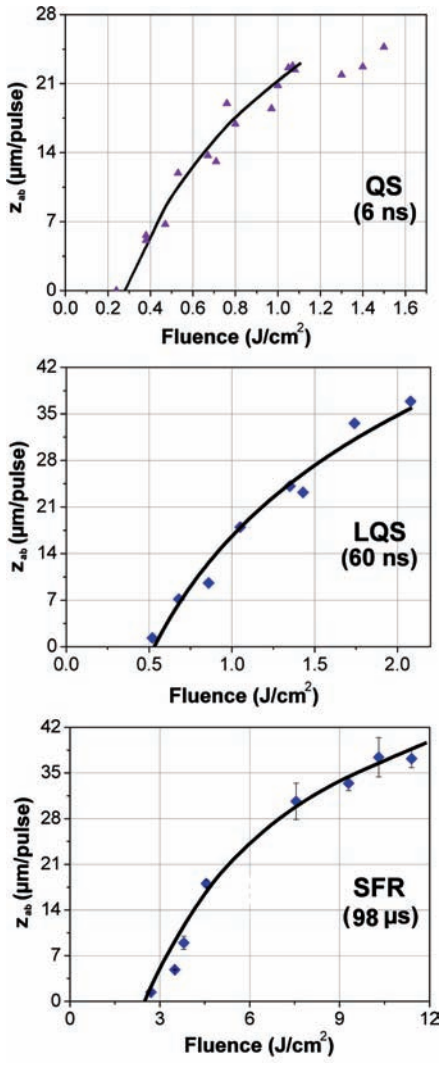

FIGURE 1. Ablation rates measured and fitting using the *blow-off* model for QS, LQS, and SFR.

Despite the previous expression of z_{ab} being referred to a vaporization-mediated ablation of homogeneous materials, its application to fit the data achieved for the present stratification provides useful information on the basic mechanisms involved.

For short pulses (QS), the logarithmic law apparently reproduces the rate increase only up to about 1 J/cm^2 (Figure 1), which allows derivation of $F_{th} = 0.28$ J/cm^2, $F_s = 0.76$ J/cm^2, and $\delta = 16.5$ μm. Above 1 J/cm^2, the data show a saturation behavior more pronounced than that estimated by the model. Furthermore, the latter significantly underestimate δ with respect to the measured value ($\delta = 27$ μm). This accelerated saturation is likely due to the occurrence of nonlinear optical absorption phenomena produced by local ionization of highly absorbing particles, which increase the typical effect of saturation due to the shielding of the expanding ablation plume.

A better agreement was achieved for the LQS and SFR. The fitting parameters of the former were $F_{th} = 0.56$ J/cm^2, $F_s = 1.51$ J/cm^2, and $\delta = 25.8$ μm. Those of the latter depended on t_L: $F_{th} = 2.2-4.7$ J/cm^2 and $F_s = 5.9-12.3$ J/cm^2, when $t_L = 50-150$ μs, respectively, which showed that the linear approximation holds over a large temporal range.

In all these cases, the ablation process is driven by water vaporization around absorbing particles, which are overheated because of their high opacity and act as photothermal converters. For black crusts, water occupies at least 60% of the irradiated volume, and it is certainly the first component to be partially vaporized, since the critical temperature of the others is much higher. Some indications about the amount of water vaporized is provided by the estimated critical energies ($\varepsilon_{cr} = F_{th}/\delta$): 170, 217, and 863−1844 J/cm^3 for QS, LQS, and SFR, respectively. Among these, only the latter is the same order of magnitude as the critical energy of water ($\varepsilon_w = C_w\Delta T + Q_w = 2591$ J/cm^3, where C_w is specific heat and Q_w is latent heat of vaporization), whereas the others are much lower.

Ablation begins with vaporization of a variable amount of water around absorbing components. An estimation of the typical radial size of the microvolume vaporized is derivable from the thermal diffusion length, $l_{th} = 2(D_w t_L)^{1/2}$ (D_w = thermal diffusivity of water): 59 nm, 186 nm, and 5.4−9.3 μm for QS, LQS, and SFR, respectively. The comparison of operative energy densities with ε_{cr} estimated enables us to make the following considerations.

SFR energy densities (10^3-10^4 J/cm^3) are compatible with the vaporization of a relevant fraction of the water that imbibes the irradiated volume, which is often noticeable to the naked eye. Conversely, the corresponding amount for short pulses (QS and LQS) can be almost negligible, but a large increase in volume is associated with the phase explosion because the heating is much more localized. For QS, the local peak pressures generated in proximity of the absorbing particles is dependent on the laser pulse duration ($P_{max} \approx t_L^{-1/2}$) and can easily reach several hundred bars. This represents a limitation for short pulses whenever uncovering very fragile or absorbing layers to be safeguarded.

The thermal conduction within the irradiated volume determines the differences between the ablation thresholds but is not the only factor. The present parametrization also shows the presence of another relevant contribution to the material removal. Both QS and LQS generate coherent pressure waves, which propagate through the irradiated volume at the speed of sound. By assuming roughly an average speed of 3000 m/s, the propagation length corresponding to 6 and 60 ns is 18 and 180 μm, respectively, which produces coherent super-

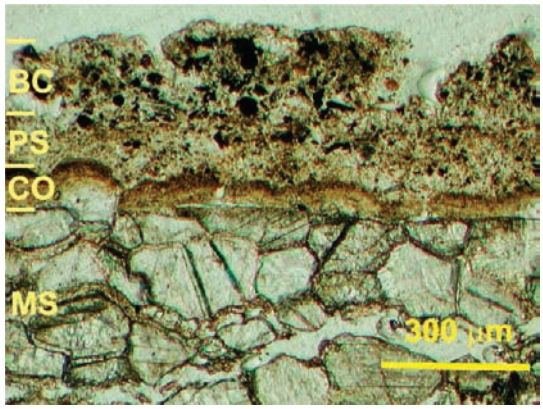

FIGURE 2. Representative stratigraphy of encrusted stones: BC, black crust; PS, pigmented scialbatura; CO, Ca-oxalates film; MS, sulfated marble substrate.

position of the point source waves and then the formation of two wavefronts propagating in inner and outer directions. The total reflection of the latter at the sample−air interface produces a rarefaction wave. This stretches the material, thus taking part in the material removal. This contribution to the ablation is called spallation. For the present samples, it is more pronounced for QS laser around F_{th}, according with the relatively low value of the latter and the high slope of the curve, but more generally the estimation of the pressure transient wavelength suggests spallation could became relevant also for LQS laser.

2.2. Gradualness and Appearance. The highest efficiency was achieved when using QS at low fluences (≤1 J/cm^2), but it rapidly saturates because of the nonlinear absorption and shielding. The optical linearity of LQS makes it more efficient than QS above 1.5 J/cm^2. Conversely, the ablation rates of SFR were decidedly lower, though the extension of the linear ablation produces higher ablation depths. The efficiency can be exploited for increasing the productivity, but in several cases, a low rate would be preferable with respect to single-shot deep ablation, which can be uncontrollable.

The main materials composing natural black crusts due to urban pollution are gypsum, quartz, black carbon, iron oxides, oily residues, other earthy materials, and minor components. However, cases of pure black crusts are rare. Art objects have undergone several treatments over the centuries, including the application of coats, such as organic binder−patinations, whitewashes, pigmented scialbaturas, and others, which nowadays must be removed for conservation and fruition issues. Figure 2 displays a representative example of multiple layers on stone, but obviously many different situations can be encountered.

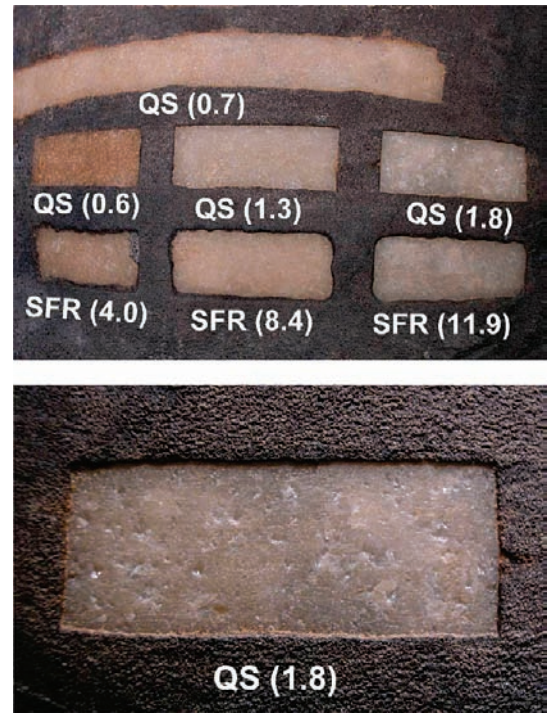

FIGURE 3. Comparative tests using QS and SFR: differences between the operative ranges. The detail shows the occurrence of visible damage induced by QS at relatively low fluence.

The strong inhomogeneity of the optical properties along the cross section of the irradiated stratification has a crucial importance in laser cleaning. In the example of Figure 2, there is an increasing diffusivity moving from the outer black crust to the inner Ca-oxalates film, and then to the sulfated stone underneath. The fluence needed to ablate the inner Ca-oxalates layer may be significantly higher than that of the black crust also due to the significant ochre content, which implies a fundamental difference between the QS and longer pulse lasers. As already described, the fluence increase of the former is limited by nonlinearity and the consequent photomechanical side effects. Conversely, the larger operative domains of LQS and especially SFR can enable a more precise control of the final degree of cleaning. This is shown by the comparative cleaning tests of Figure 3, which were carried out on a stone fragment from the façade of Florence's Cathedral whose stratigraphy is that of Figure 2.

The higher controllability associated with longer pulses concerns the final phase of the cleaning, whereas the gradualness of the removal of the different temporal regimens through the stratification strongly depends on composition and microstructure of the strata.

Most problems of yellow-orange appearances after the laser cleaning of marbles are due to residues of iron oxides, Ca-oxalate films with pigment loads, organic substances, and other pigmented components of the stratification. The attribu-

tion of yellow appearance to residues of materials coming from the stratification has been pointed out also by other authors.[7] However, deeper degrees of cleaning using higher fluences typically provide lighter appearances and colder color hues. Often, the usual operative fluences of QS lasers (0.1−1 J/cm^2) are insufficient for removing the last pigmented film in proximity to the whitish marble substrate, whereas this can be achieved at the operative fluences of longer pulses (2−8 J/cm^2). The damage thresholds of LQS and SFR are significantly higher than that of QS. Thus for example, for aged white marbles, we have typically measured 3−4, 20−30, and 1−1.5 J/cm^2, respectively.

In addition to pigmented residues, the case of yellow hues well beneath the stone surface are also encountered. This condition is usually observed for gypsum, stucco, plaster, and porous stone treated in the past with oily substances. Comparisons between different lasers and mechanical cleaning have shown very similar chromatic results. The final appearance does not depend on the cleaning method in such cases.

To complete the picture, we also investigated the possible occurrence of staining associated with laser ablation. Cleaning tests on samples prepared by applying pure black carbon or black crust scraped from genuine marble artifacts were carried out. For all three lasers used, the ablation of black carbon in dry conditions produced grayish staining, which was more pronounced at the lowest fluences and gradually disappeared at the higher fluences. No relevant staining effects were observed in water-assisted conditions, apart from very light grayish discoloration at low fluences. Similar effects were noted for the genuine crust, with the difference that the color of the stains for QS and LQS was pale yellow rather than grayish, as for SFR. However, fluence increase and water assists effectively prevented any discoloration effect.

2.3. Stone Case Study. The *Architrave* of San Ranieri is a bass relief of Roman origins (reused and integrated during the Late Middle Ages) that decorates the north portal of the Cathedral of San Ranieri in Pisa. The entire cleaning of the carved parts (about 6 m^2) was carried out using laser ablation.

The stratification was similar to that reported in Figure 2, whereas the present substrates are Greek marble (main central relief) and local marble of San Giuliano (top and bottom integrations).

The state of conservation of the artwork was very serious. The hard stratification to be removed lay on sulfated marble substrate presenting deep decohesion effects. This difficult situation, along with some preliminary tests, led us to select the laser technique and to optimize an overall treatment using the SFR. The operative fluences were relatively high (up to 7−9 J/cm^2, 80 μs) due to the high reflectance and hardness of the scialbaturas and Ca-oxalates layers. The QS was found to be too invasive for the complete removal of the sulfated surface coats.

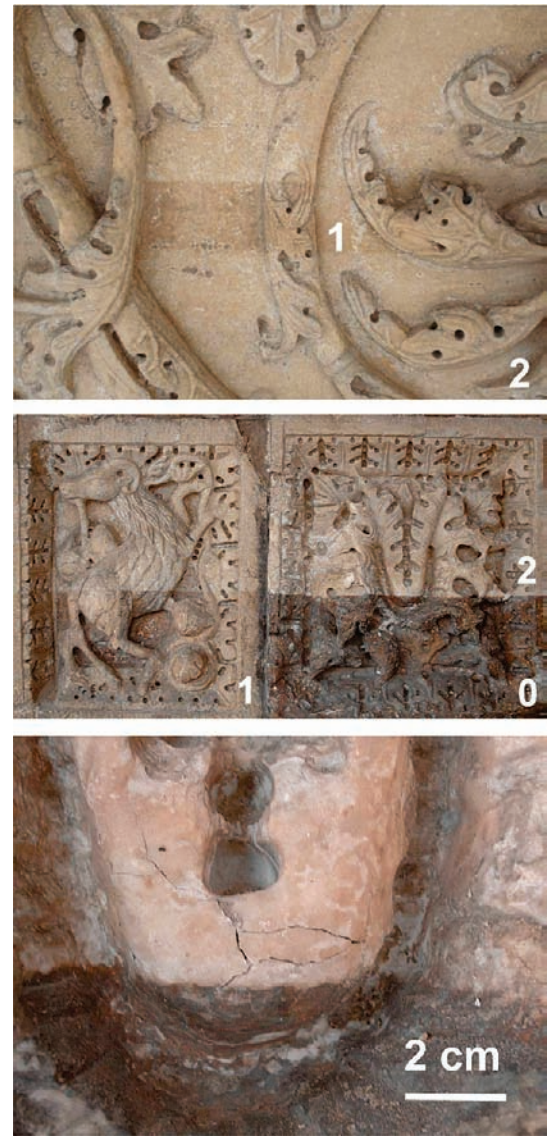

FIGURE 4. *Architrave* of San Ranieri, Pisa. Examples of selectivity and gradualness of the SFR: (0) before cleaning; (1) early degree of laser cleaning; (2) final degree of laser cleaning. The detail (bottom) shows the safeguard of the marble surface even in cases of strong decohesion.

Details of the relief during the laser cleaning are shown in Figure 4. The early degree of cleaning (1), which was achieved with fluences around 5 J/cm^2, was considered unsatisfactory, since a significant amount of sulfated residues of the stratification was still present. The laser was therefore set at a higher fluence (about 8 J/cm^2), in order to achieve a deeper cleaning. Stratigraphic diagnostics and colorimetric controls allowed assessment of a deeper removal and the safeguard of the most internal Ca-oxalate film (whewellite).

A particular situation was found on the genuine Roman part, where the SFR was not able to remove some very dark spots that were identified as residues of biological attacks. The associated ramified and tenacious microstructures did not permit a sufficient degree of removal by means of the slow vaporization-mediated ablation of the SFR. The problem was solved using the most intensive photomechanical coupling of the QS.

3. Metals

As already mentioned, the milestone in metal cleaning using laser ablation was the study of Ghiberti's *Porta del Paradiso*,[4] the restoration of which will be completed at the end of this year (Figure 5). Here, we summarize the general physical criteria and extend the laser approach to other metal surfaces.

3.1. "Semi-infinite" and "Negligible" Metal Thickness. The high reflectance of metals (R_m) is associated with an extremely high absorption coefficient. The light is dissipated in a nanometer-scale depth, which makes the thermal conduction and hence pulse duration of critical importance. For this reason, it is appropriate to approach the cleaning of metals by starting from the thermal features of laser−metal interaction.

The one-dimensional thermal conduction theory provides estimations of the temperature rise $\Delta T(z,t)$ in a metal slab with a thickness l. By consideration of the conditions in which the thermal conduction of the adjacent materials is negligible, the temperature rise produced by the absorption intensity $I_a(t) = (1 - R_m)I_L(t)$, where $I_L(t)$ is the incident laser intensity, is the following:[8]

$$\Delta T(z,t) = \frac{1}{K_m}\sqrt{\frac{D_m}{\pi}}\left\{\int_0^t I_a(t-\tau)\frac{e^{-z^2/(4D_m\tau)}}{\sqrt{\tau}}\,d\tau + \sum_{n=1}^{\infty}\int_0^t \frac{I_a(t-\tau)}{\sqrt{\tau}}\left[e^{-(2nl-z)^2/(4D_m\tau)} + e^{-(2nl+z)^2/(4D_m\tau)}\right]d\tau\right\} \quad (1)$$

where K_m and D_m are the thermal conductivity and diffusivity of the metal, respectively. $D_m = K_m/(\rho_m C_m)$, where ρ_m and C_m are density and specific heat of the metal, respectively.

The first term in eq 1 represents the solution to the semi-infinite medium, while the sum accounts for the reflection of the thermal wave at the interfaces. If $l_{th} < l$, the first term represents a good approximation, whereas the second increases for $l_{th} > l$, that is, $t_L > l^2/(4D_m)$, until it produces a homogenization of the temperature inside the slab when $l_{th} \gg l$.

Conversely, if the heat generated by the irradiation of the metal film is massively transferred to the underlying low conductivity (K_i) substrate, temperature estimations can be achieved by considering the surface−layer approximation:

$$\Delta T(z,t) = \frac{I_a}{bK_i}\left[2b\sqrt{\frac{D_i t}{\pi}}\,e^{-\eta^2} - (1+bz)\mathrm{erfc}\,\eta + e^{b(z+D_i b t)}\,\mathrm{erfc}(\eta + \sqrt{D_i t})\right] \quad (2)$$

where $\eta = z/[2(D_i t)^{1/2}]$, $b = r_i C_i/C_{m1}$, and C_{m1} is the thermal capacity per unit area of the gold film.

In practical applications, eq 1 can be used to estimate the temperature rise in metal films with thickness above some micrometers, such as for amalgam gilding, gold and silver inlays, and silver objects. In contrast, eq 2 is suitable for gold leaf gilding, of which the typical thickness is 100−500 nm. These considerations derive from the estimation of l_{th}. Thus, for example, if we assume a gold film (K_m = 286 W/(m °C)), D_m = 1.23 cm^2/s) with an average thickness of about 6 μm, as is that of the *Porta del Paradiso*, l_{th} = 1.7, 5.9, and 140 μm for QS (6 ns), LQS (70 ns), and SFR (40 μs), respectively. For both the QS and LQS, the metal film behaves as a semi-infinite medium since the reflection at the internal interface is negligible. Conversely, for SFR laser heating, the thermal wave undergoes many reflections, which produce an almost constant temperature along the thickness. The assumption of negligible conduction outside the film aims to include the most delicate cases where the film is detached from the substrate. Conversely, disregarding the conduction of the layer beneath the gold leaf is too unrealistic since $l_{thi} \gg l$ in any case.

Equation 1 shows that the temperature of a metal significantly increases when the laser pulse duration decreases: $\Delta T(0,t_L) \approx t_L^{-1/2}$, as is also evident from the decrease of l_{th}. Thus, the cleaning of low-melting point metals with a QS is very harmful. At the same time, eq 1 indicates significant temperature rises at the typical operative fluences of the SFR due to the contribution of the reflection term. Thus, for example, by assuming a constant F_a = 150 mJ/cm^2, eq 1 estimates a peak temperature of about 450 and 170 °C for the QS and the LQS, respectively. Instead a realistic absorption fluence for the SFR is around 1 J/cm^2, which would involve a homogeneous temperature rise in the film up to 240 °C lasting for a longer time.

These are the basic reasons that led us to propose LQS for cleaning amalgam gilding, gold and silver inlays or laminas, and silver alloy objects. A general optimization rule for metal films with a thickness on the order of micrometers is provided by the condition $l = l_{th}$ ($t_L = l^2/(4D_m)$). By using operative fluences of 0.5−1 J/cm^2, one can achieve safe laser ablation without any relevant risk of micromelting.

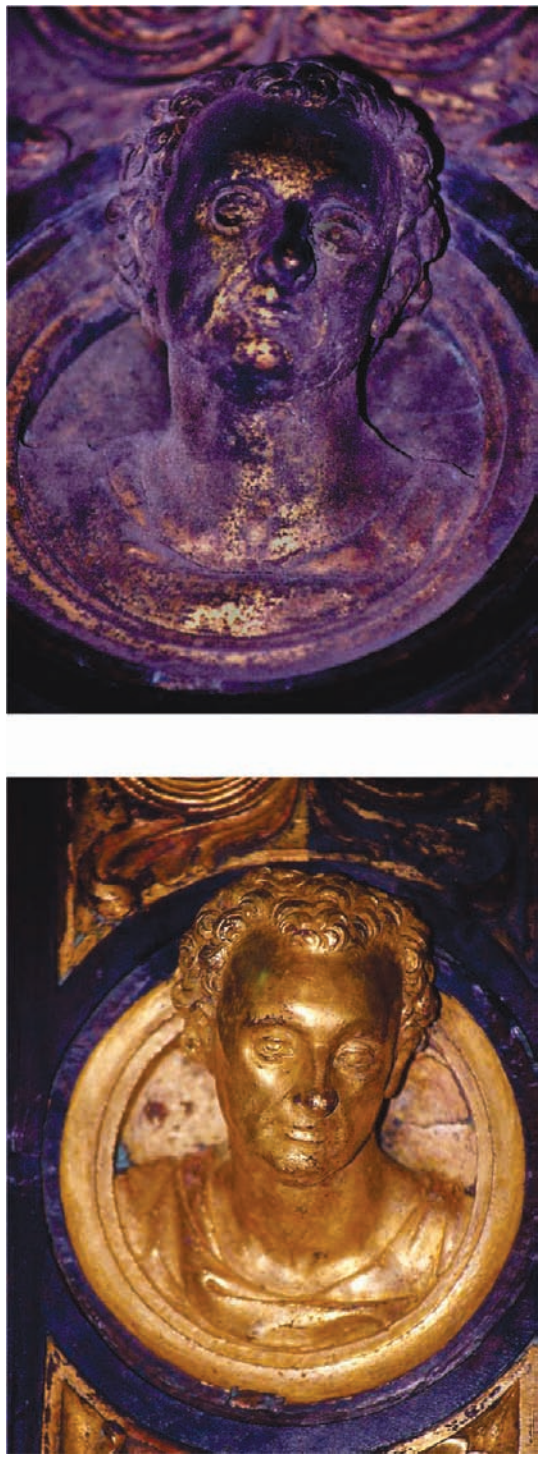

FIGURE 5. Lorenzo Ghiberti's *Porta del Paradiso*: a *tondo* before and after LQS laser cleaning.

Conversely, the thermal analysis (eq 2) for gold leaf suggested a limited application perspective for the QS and LQS (though not ruled out), because the presence of the gold layer produces a strong concentration of the laser heating within the leaf and immediately underneath, which could easily destroy the gilding. The SFR was found to be more suitable in this case. It can also be used on thick metals; however the ablation is so effective to produce satisfactory degrees of cleaning only in rare cases.

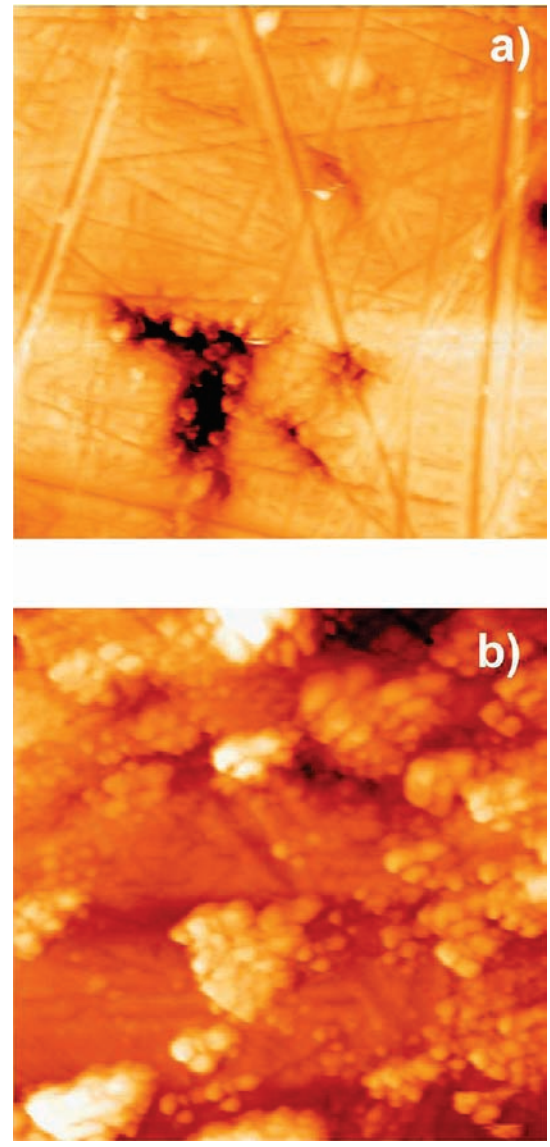

FIGURE 6. Atomic force microscopy of amalgam gilding (a) before treatment ($10 \times 10\ \mu m^2$) and (b) after ablation of malachite in dry conditions ($3 \times 3\ \mu m^2$).

3.2. Ablation Dynamics and Degree of Cleaning of Metals. Let us focus on "thick" gilding, silver, and other cases in which $I > I_{th}$, whereas laser ablation involved in the cleaning of gold leaf using SFR is mainly driven by slow vaporization, as described above.

In metal cleaning, water assists are even more important than for stones, since gold and silver surfaces can undergo serious staining effects. Figure 6 shows nanoscale structures following laser ablation in dry conditions of malachite on a synthetic amalgam gilding sample. They were generated by redeposition of ablation products. For silver also the direct oxi-

dation associated with temperature gradients of some hundreds of degrees can occur.

Laser cleaning using the LQS can be described in accordance with the inhomogeneous vaporization and spallation dynamics mentioned above with the addition of a further contribution provided by the transient heating of the metal surface. The latter easily exceeds the vaporization threshold of water, thus generating expansion and a pressure wave at the bottom of the irradiated volume, which can significantly amplify the efficiency of the material spallation.

Especially in the present case of relatively low operative fluences, the thickness of the water-assists layer is very important. In principle, water should simply imbibe the material to be removed, since thicker layers reduce the intensity of the rarefaction wave and increase the acoustic impedance against material ejection. On the other hand, the case of underwater irradiation can also have certain practical applications in metal cleaning.

Underwater irradiation of an absorbing stratification generates an intensive microexplosion that releases a strong recoil stress against the target. Above a given threshold, the latter can mechanically fragment or erode the stratification. Furthermore, as is well-known, an intense underwater explosion also generates the expansion of a cavitation bubble, the subsequent collapse of which produces a water jet, which releases a second mechanical stress against the target. At sufficiently high fluences, a sequence of two to three cavitation cycles could be triggered by the single laser pulse.

The peak pressure associated with the early microexplosion is closely dependent on the pulse duration. As for black particles in gypsum crusts, $P_{max} \approx t_L^{-1/2}$, whereas the water hammer pressure of the collapse depends on the speed of the water jet (v_j): $P_{wh} \cong \rho_w c_w v_j$, where ρ_w is the density of water and c_w is its sound speed. Typical collapse speeds $v_j = 10-100$ m/s produce a water hammer pressure $P_{wh} \cong 750-1500$ bar, which certainly contributes to the material removal.

3.3. Metal Case Studies. To provide some example applications, we selected the recent restoration work of a small silver relief (15×25 cm^2) by Guglielmo della Porta (crafted around 1550), the Roman silver coin Treasure from Rimigliano (Livorno), and Donatello's *David*. The former represents the very general problem of tarnished silver, in which the thin sulfur-rich layer is intimately bound to the metal, which makes this case more difficult than the removal of deposits or varnishes. For the restoration of the coin Treasure, we applied underwater laser cleaning for the first time. Lastly, the *David* represents the most recent conservation problem of oil gilding solved using laser ablation.

FIGURE 7. Detail (10 cm vertical size) of a silver relief by Guglielmo della Porta (XVIth century) during laser cleaning. Reproduced by permission of Nardini Editore, Florence.

As for gilded bronzes, the irradiation of tarnished silver in dry conditions produces unacceptable discoloration effects. For this reason, cleaning tests using the LQS ($0.5-1$ J/cm^2) were carried out under water-assisted conditions, with the addition of air, nitrogen, or argon flux. None of them enabled us to completely solve the problem of redeposition, even though argon assists minimized such a side effect. However, it was observed that a minimal mechanical action with wet cotton or other material easily removes the redeposition film, which makes gas assists redundant. However, a finishing of this type must be performed soon after the laser treatment, since the residues rapidly react with the substrate in a way that makes the removal very difficult after a few hours.

Laser cleaning of tarnished silver is quicker than traditional methods, including preliminary treatments with acetone and distilled water and then chemical and mechanical actions using sodium carbonate solutions. The LQS allows self-terminated ablation within a sufficiently wide operative range, before the occurrence of direct oxidation and micromelting. The final appearance (Figure 7) is similar to that provided by traditional methods with the difference that the strong abrasion involved in the latter is more invasive.

The Treasure from Rimigliano was an agglomerate of about 3500 silver-alloy Roman coins (230–260 AC). The archeologists decided to detach about 300 coins from the block in order to clean them for a thorough classification. Furthermore, they decided to clean the coins at the top of the agglomerate for exhibition purposes.

FIGURE 8. The Treasure from Rimigliano: detail (top) and general view (bottom) during underwater laser cleaning using the LQS and the SFR.

After assessing that it was practically impossible to remove safely the hard and thick mineral stratifications using laser irradiation in air, we decided to test underwater cleaning. The result were better than expected. Both the LQS and SFR provided very satisfactory results without any alteration of the natural surface texture and, more importantly, much better than those achieved with traditional mechanical cleaning using a piezoelectric ablator. Figure 8 shows the first cleaning test (top) and a general view of the Treasure after being partially cleaned (bottom).

Figure 9 reports the cavitation cycles that were imaged in operative conditions (LQS, 120 ns, 1.5 J/cm) using a time-resolved laser shadowgraph setup. This confirmed the previous description of underwater cleaning. Furthermore, pressure measurements using a needle hydrophone were conducted, which showed that both lasers induced phase explosion and water hammer pressure peaks of comparable amplitude. For the LQS, the former was more intense than the latter, whereas the situation was inverted with the SFR. In both cases, the ablation process was self-terminated at the reflecting metal surface.

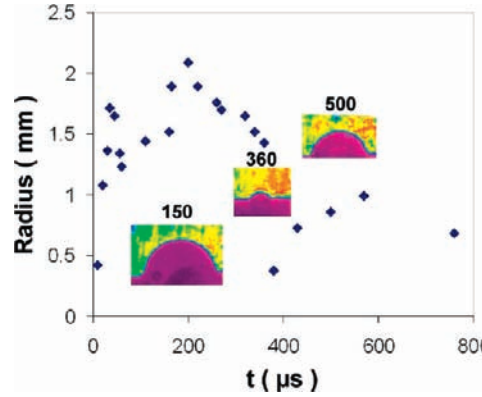

FIGURE 9. Time evolution of the cavitation bubble (LQS, 120 ns, 1.5 J/cm^2): radius measured using time-resolved laser shadowgraph (images at three different delays are also shown).

The restoration work recently performed on Donatello's *David* was aimed at removing a brown coat applied in the past. Thorough XRD, FT-IR, and gas-chromatography analyses enabled us to assess that this coat was composed of a mixture of quartz, gypsum calcite, Ca- and Cu-oxalates, Al-silicates, a pigment load of Fe-oxides, and carbon black in organic binder (linseed oil and colophony). The thickness was quite variable up to 100 μm. Similar intentional layers have been found in previous restoration work on other Florentine artworks.

The coat strongly altered the fruition and was considered unsafe for the future conservation of this unique masterpiece. Furthermore, it completely covered the original oil gilding decorations (Figure 10). In accordance with basic concepts already discussed, the cleaning of the latter was carried out using the SFR laser at maximal irradiation fluences of around 2 J/cm^2, which were sufficient to produce thermal alteration and a safe removal of the organic binder—patination. This allowed recovery of the relicts of the original gilding, which were abundant on the hair (Figure 10) and minimal in the lower part (Goliath's beard). Furthermore, laser irradiation was also used in order to effect a preliminary disaggregation of the patination in nongilded zones before sodium carbonate poultices and then mechanical removal.

4. Wall Paintings

The cleaning of painted surfaces represents a big challenge for laser cleaning. Studies were conducted on easel paintings for which excimer (mainly KrF*, 248 nm) and free running Er:YAG (2.94 μm) lasers have been proposed. Most of the materials, in particular varnishes, strongly absorb at the wavelengths of these two lasers ($\delta \leq 1$ μm), which can therefore be used for lightening varnishes darkened by aging. However, 248 nm and 2.94 μm are also strongly absorbed by paint layers and

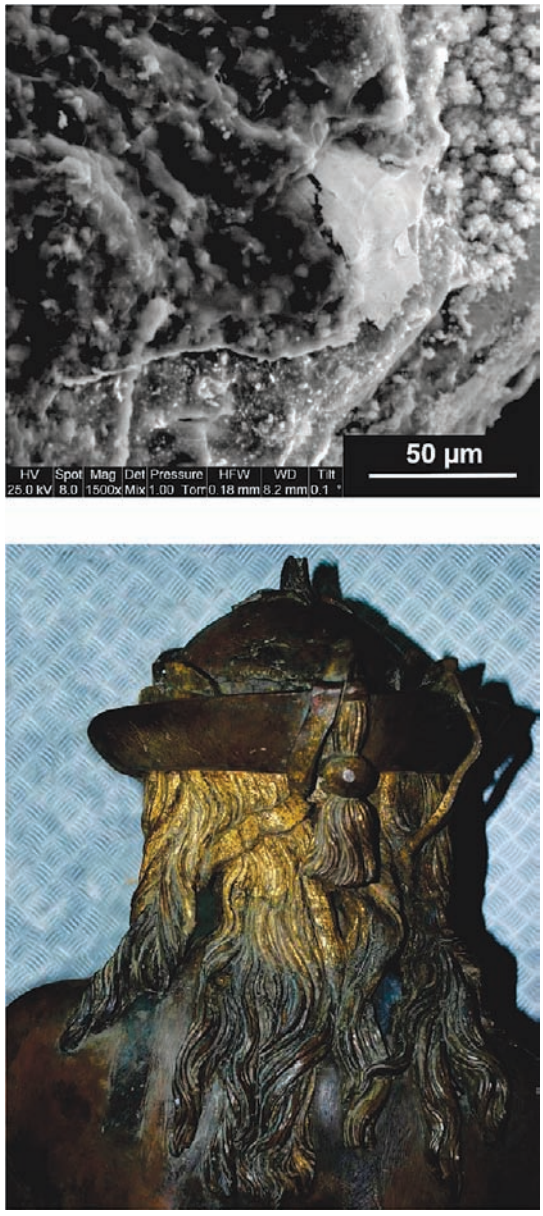

FIGURE 10. Donatello's *David*: SEM of oil gilding coated by patination applied in the past (top) and a view of the hair after laser cleaning (bottom). The former is reproduced by permission of Giunti Editore, Florence.

hence require a careful control of the irradiation fluence and ablation depth. This is a different approach with respect to the idea of developing self-terminated processes.

A systematic laboratory investigation was carried out on frescoed samples in order to assess the potential of QS (6 ns), LQS (120 ns), and SFR (40−50 μs) for the solution of specific cleaning problems. Several pigments were used, including red and yellow ochre, raw sienna, green earth, azurite, ultramarine and Egyptian blue, malachite, verdigris, and zinc white.

We determined the damage thresholds of all these pigments for the three pulse durations available; various cleaning problems were then simulated by applying a layer of black carbon, white and dark limewashes, or dark Paraloid to the paint samples. Moreover, we have learned from practical experience that limewashes were often applied on existing dark deposits. Thus, samples with whitewash on black carbon were realized in order to simulate a real situation of this type.

None of the pigment investigated underwent discoloration in water-assisted conditions. The damage was essentially represented by partial or total ablation of the paint layer. This is very important, since prepared paint layers were weaker than genuine ones because of the weak carbonatization. Thus, the damage thresholds are expected to be higher in practical cases.

As for stones and metals, also for wall paintings, we found that the LQS and SFR provide larger operative ranges and more discrimination potential than the QS. The damage thresholds were fairly high (between 0.7−0.9 J/cm^2 and 3.5−5 J/cm^2 for LQS and SFR, respectively) and therefore permit the safe removal of black carbon, dark limewash, and dark Paraloid. The removal of pure whitewash is possible only in a few cases.

Conversely, whitewash on black carbon represents the best situation. A very effective ablation of the stratification was achieve with LQS at only 0.2 J/cm^2. The SFR irradiation provided the selective removal of whitewash at 2 J/cm^2, while the black layer underneath was ablated at a higher fluence (3 J/cm^2).

The process involved in the removal of whitewash, which is a not absorbing layer, is always a spallation that is induce by heating the absorbing layer underneath. It can be referred to as "secondary spallation" in order to distinguish it from the primary spallation introduced above.

Secondary spallation is not a laboratory exercise. We are finding that it represents a very effective process, which plays a fundamental role in practical cases of limewash removal, as well as in other situations such as those of the following cases.

4.1. Wall Painting Case Studies. Laser cleaning has been successfully tested and consequently extensively applied to uncover the wall paintings of the *Sagrestia Vecchia* (1446−1449) and the *Cappella del Manto* (1370) in Santa Maria della Scala, Siena, those of the donjon of the Castle of Quart (Late Middle Age), in Aosta Valley. The stratifications to be removed were aged Paraloid with residues of a previous limewash for the *Sagrestia Vecchia*, whitewash for the *Cappella del Manto*, and limewash with the addition of animal glue for the paintings of the Castle of Quart. In all these cases, we found a black layer of carbon deposits (Figure 11) under

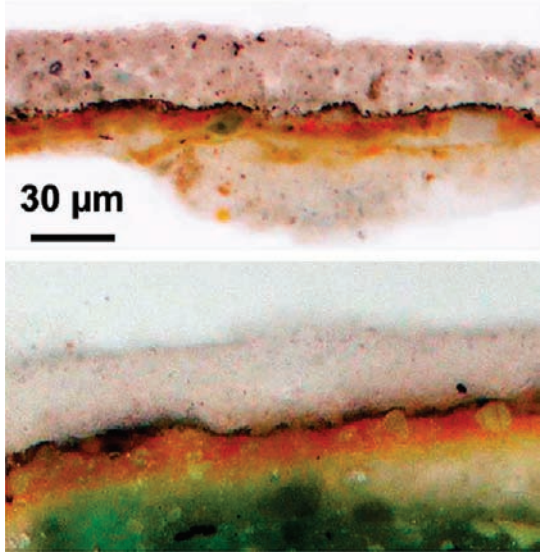

FIGURE 11. Stratigraphies of the wall paintings in the *Sagrestia Vecchia* (top) and the *Cappella del Manto* (bottom). From top to bottom: limewash (with Paraloid for the former), carbon deposits, iron-based paint layers.

FIGURE 12. *Sagrestia Vecchia*, Siena: comparison between traditional cleaning (two angels on the left) and LQS cleaning (angel on the right partially cleaned).

the whitish layers to be removed, which favored ablation by secondary spallation.

The cleaning results achieved are surprisingly good; indeed they are better than those of any other alternative technique tested (Figure 12−14). The dark stratification on the face of the angel in Figure 12 (*Sagrestia Vecchia*) was removed using the LQS at 0.7 J/cm^2. The ablation process self-terminated, thanks to the high reflectance of the iron pigments and calcite of the paint layers uncovered. The early damages were observed at 1.5 J/cm^2. As expected, this value is somewhat higher than those of the laboratory samples.

Two different cleaning levels are shown in Figure 13 (*Cappella del Manto*). They were achieved by using the SFR (bottom) and the SFR followed by LQS (top), respectively. A residual veil of the ancient carbon deposits was visible after the former treatment, which was completely removed with a further irradiation with LQS.

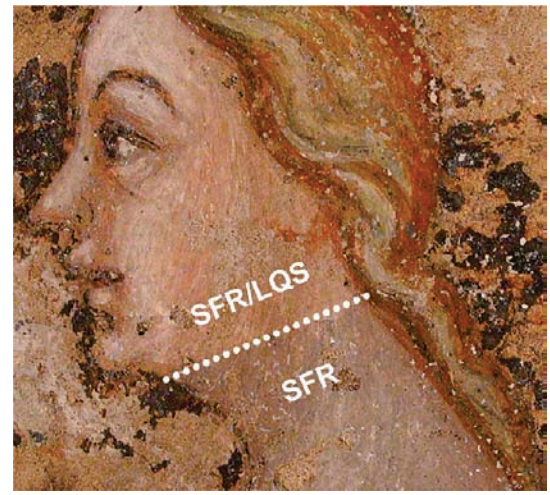

FIGURE 13. *Cappella del Manto*, Siena: two-step laser cleaning treatment.

FIGURE 14. Donjon of the Castle of Quart: SFR laser cleaning on red and black pigments.

The cleaning of the Gothic Linear Style paintings of the Castle of Quart was also approached by a combined use of the LQS and SFR. The former was effective on lead white-rich paint layers, whereas SFR was used on ochre and black carbon overpaint (Figure 14). This result is either really impressive or a kind of paradox, since laser ablation is typically used for removing "black" from "white". The SFR allows removal of a whitish layer (lime *scialbatura*) from a black pigment.

5. Conclusions

In this work, we have shown that a suitable selection of Nd:YAG laser pulse duration and irradiation conditions can

significantly extend the potential of laser cleaning. A set of successful results have been presented for stones, metals, and wall paintings that evidence the achievement of improved degrees of selectivity and control of the ablation processes.

The methodological criteria introduced for the different typology of artifacts are intended as starting points for optimizing the laser cleaning procedures rather than as general recipes. In practical applications, preliminary tests should always be carried out in order to assess the phenomenology and therefore adapt what is stated here to the specific problem under study, taking into account all its unique features. Furthermore, since laser cleaning is very rarely applied as stand alone, also the combination with chemical and mechanical techniques should be suitably pondered in order to minimize the invasiveness and improve the result of the cleaning treatments.

BIOGRAPHICAL INFORMATION

Salvatore Siano graduated in physics from the University of Florence. He leads a research group at the Applied Physics Institute-CNR of Florence that works on the development and application of laser and optoelectronic techniques for the study and conservation of cultural heritage. He is the person in charge of several research projects on the topic and is involved in the application of the laser techniques to important restoration works of famous masterpieces.

Renzo Salimbeni graduated in physics from the University of Florence and is Director of the Applied Physics Institute-CNR of Florence. His scientific activity has been dedicated to laser technologies and their application in various fields. He has been in charge of several research projects devoted to the conservation of the cultural heritage.

FOOTNOTES

*E-mail: S.Siano@ifac.cnr.it.

REFERENCES

1 Asmus, J. F.; Murphy, C. G.; Munk, W. H. Studies on the interaction of laser radiation with art artifacts. In *Developments in laser Technology II*; Weurker, R., Ed.; SPIE: Bellingham, WA, 1973; Vol. 41, pp 19—30.

2 Georgiou, S.; Anglos, D.; Fotakis, C. Photons in the service of our past: lasers in the preservation of cultural heritage. *Contemp. Phys.* **2008**, *49*, 1–27.

3 Margheri, F.; Modi, S.; Masotti, L.; Mazzinghi, P.; Pini, R.; Siano, S.; Salimbeni, R. Smart Clean: a new laser system with improved emission characteristics and transmission through long optical fibres. *J. Cult. Heritage* **2000**, *1*, S119—S123.

4 Siano, S.; Salimbeni, R. The gate of Paradise: Physical optimization of the laser clearing approach. *Stud. Conserv.* **2001**, *46*, 269–281.

5 Salimbeni, R.; Pini, R.; Siano, S. A variable pulse width Nd:YAG lasser for conservation. *J. Cult. Heritage* **2000**, *4*, 72s–76s.

6 Bromblet, P.; Labouré, M.; Orial, G. Diversity of the cleaning procedures including laser for the restoration of carved portals in France over the last 10 years. *J. Cult. Heritage* **2003**, *4*, 17s–26s.

7 Pouli, P.; Fotakis, C.; Hermosin, B.; Saiz-Jimenez, C.; Domingo, C.; Oujja, M.; Castillejo, M. The laser-induced discoloration of stonework: A comparative study on its origins and remedies. *Spectrochim, Acta, Part A* **2008**, *71*, 932–945.

8 Siano, S.; Grazzi, F.; Parfenov, V. A. Laser cleaning of gilded bronze surfaces. *J. Opt. Techn.* **2008**, *75*, 419–427.